

## Untersuchung des Einflusses von Wirbelstrukturen auf Transportprozesse an fluiden Phasengrenzen

### Investigation of the influence of vortex structures on transport processes at fluidic interfaces

**Sophie Rüttinger, Marko Hoffmann, Michael Schlüter**

Institut für Mehrphasenströmungen, Technische Universität Hamburg,  
Eißenendorfer Straße 38, 21073 Hamburg

Mehrphasenströmungen, Particle Image Velocimetry, Laser-induced Fluorescence,  
Stofftransport

Multiphase Flows, Particle Image Velocimetry, Laser-induced Fluorescence, mass transfer

#### Abstract

In applications of process engineering, the in-depth knowledge on transport processes is crucial for the design and optimization of apparatuses which are used in the chemical, pharmaceutical, biological and food industry. The connection between the flow structure and mass transfer processes has not been exhaustively researched yet. Process design is still based on empirical correlations which use the dimensionless Sherwood number to describe the mass transfer as a function of hydrodynamics (Reynolds number) and material system (Schmidt number). These correlations are deduced from lab-scale experiments on single bubbles. Even though there is a large body of literature on multiphase reactors like bubble columns, jet loop reactors or stirred tank reactors, the underlying principles of hydrodynamics and mass transfer close to fluidic interfaces are not yet fully understood.

To better understand these principles, a study is designed to investigate the influence of vortices on hydrodynamics and mass transfer at a single bubble which is fixed in place. This experimental approach is chosen to observe how vortices which can arise due to bubble wakes, flow around reactor installations, and of course turbulence change the boundary layer dynamics and the local velocity distribution around a single bubble. For this purpose, Particle Image Velocimetry and Laser-Induced Fluorescence techniques are used to get information on both velocity and concentration fields.

It turns out that the vortices generated in this study significantly influence the bubble wake and thus, the crossmixing behind the bubble. Even though it is shown that the vortices also peel off the concentration boundary layer, there is no significant change in the over-all mass transfer. It is therefore concluded that the mass transfer from a dispersed phase into a bulk phase is limited to a viscous sublayer (as it is known from the boundary layer theory) which is not influenced by vortices in a non-turbulent flow.

#### Introduction

The principle of many multiphase industrial applications like absorption, oxidation or aeration is the rising of a dispersed gas phase through a continuous liquid phase, whereby mass transfer takes place from one phase into the other. When a bubble rises through a stagnant liquid, a complex interdependency between the bubble rising velocity and rising path, the bubble shape, the wake structure and, finally, the mass transfer occurs. The connection between these phenomena is still not completely understood.

By now, the film theory (Lewis and Whitman, 1924) is applied to describe the mass transfer from a gas bubble into the liquid bulk phase. Assuming that the transport resistance is limited to the liquid phase, a film is considered to arise close to the interface, where the concentration changes from the value at the interface (where a phase equilibrium is assumed) to the value within the bulk phase. Within this film, only diffusion occurs according to Fick's law:

$$j_i = -D \cdot \frac{dc_i}{dx}$$

Hereby, the index  $i$  depicts the species which is transferred across the interface. This is illustrated in figure 1.

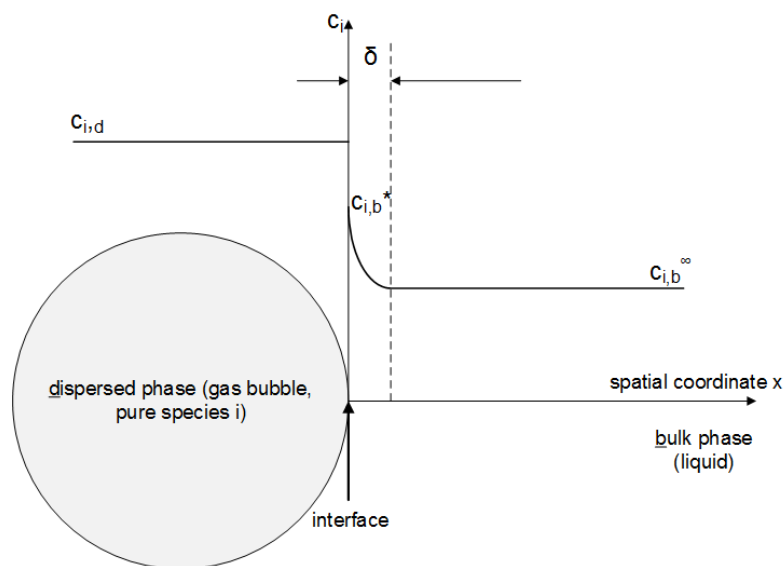


Fig. 1: Schematic illustration of mass transfer from a gas bubble into a liquid bulk phase.

The guiding question of this study is, whether vortex structures can change the mass transfer described above. Vortex structures occur when many bubbles rise through the liquid, and the bubble wakes from the preceding bubbles approach the following bubbles. To reduce the level of complexity, the vortex structures are produced by the flow around a circular cylinder upstream the bubble. Detailed velocity (PIV) and mass transfer (LIF) measurements are possible due to the fact that the investigated bubble is kept in place and shape by a cap. From the data, tangential velocity profiles close to the bubble interface are determined, as well as local Sherwood numbers.

## Experimental Set-Up

The experiments are conducted in a duct made from acrylic glass with a square-shaped cross section (see figure 2). Within the duct, a single bubble ( $\text{CO}_2$ ) is held in place and in shape by a cap. This enables experiments for a comparably long period (20 s) and with different, also lower Reynolds numbers. By means of a hypodermic needle, the bubble is injected into the liquid flow of demineralized water, which is seeded with tracer particles, through a septum. The illumination is carried out by a Nd:YLF PIV laser, which excited the fluorescent dye coated tracer particles. Images are taken in equidistant frame rate by means of a high-speed camera (see table 1). The camera is equipped with a bandpass filter which makes it possible to only record the fluorescence light of the tracer particles. Thus, no reflections of the systems are recorded, and furthermore, the camera is protected from the highly

energetic laser light. Further information on the parameters of the high-speed PIV measurements can be found in table 1 and in Rüttinger et al., 2018.

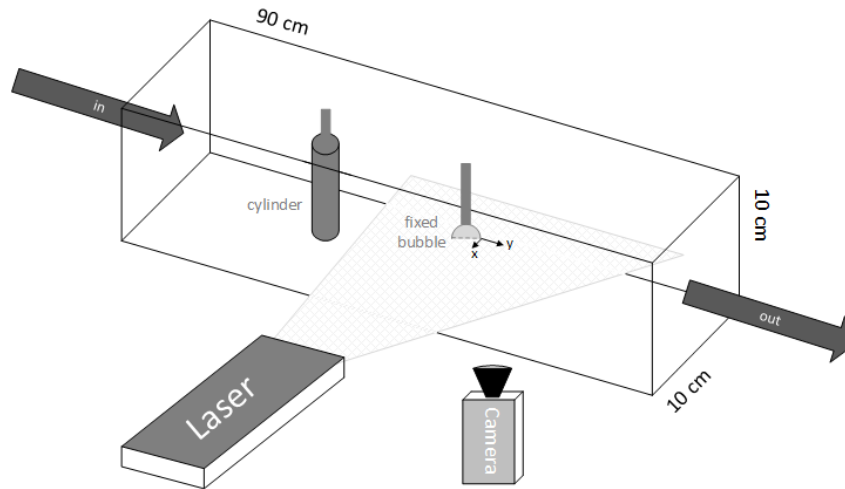


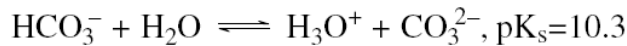
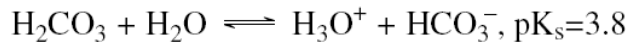
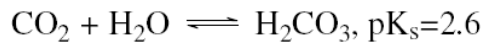
Fig. 2: Experimental set-up (Rüttinger et al, 2018).

Upstream the bubble, a cylinder is positioned. The cylinder diameter (2 cm) is approximately four times the bubble diameter (5 mm), which leads to a Reynolds number of the cylinder of  $Re_{cyl} \approx 480$ . This is chosen since with this parameter selection, the diameters are of the same scale, but the vortex street produced by the cylinder is already instationary and transient in shear layers (Zdravkovich, 1997). In this study, the distance between the cylinder and the bubble is  $a=5.5$  cm and both bubble and cylinder have a staggered configuration. The dimensionless distance is  $L^*=a/d_{cyl} = 2.75$ . For this value, wake interaction is known to occur for the flow around two cylinders (Sumner, 2010).

Table 1. Parameters of 2D high-speed Particle Image Velocimetry (PIV) experiments.

Parameters	Settings
Camera	PCO dimax HS2 (PCO AG, Kelheim, Germany), 1400 × 1000 Px <sup>2</sup> , 12 bit
Objective	Zeiss macro planar 2/50 mm
Bandpass Filter	ILA_5150 GmbH, center wave length 590 nm ± 2 nm
Laser	Quantronix Darwin-Duo-100M, Nd:YLF (Quantronix Inc., Hamden, CT, USA), total energy > 60 mJ, average power at 3 kHz > 90 W
Seeding Particles	PS-FluoRed-Fi203, monodisperse 3.16 µm, abs/em = 530/607 nm (MicroParticles GmbH, Berlin, Germany)
Frame Rate	500 fps
Acquisition Time	20 s
Number of Images Processed	10,000
Spatial Resolution (vector-to-vector spacing)	0.36 mm (24 Px)
Temperature	20 ± 1.5 °C
PIV Data Processing Software	PivView 3.60 (PivTec GmbH, ILA_5150 GmbH, Aachen, Germany)

The same set-up which is shown in figure 2 and described above is used for LIF experiments. For this purpose, fluorescent dye (Sodium Fluorescein) is added to the liquid flow. When CO<sub>2</sub> is transferred from the gas bubble into the liquid bulk phase, a certain amount of it reacts in an acidic reaction with the water:



For this study, only the first two reactions are of interest. They lead to a local pH change, which changes the fluorescence intensity of the dye by a quenching effect. This means that regions of high CO<sub>2</sub> concentration appear darker on the LIF images (less fluorescence), while regions of low CO<sub>2</sub> concentration appear brighter (more fluorescence). The Stern-Volmer equation makes it possible to correlate between the fluorescence intensity (in this case, grey levels) and the concentration of the fluorescence quencher (CO<sub>2</sub>):

$$\frac{I_0}{I_Q} = 1 + K_{SV} \cdot c_Q$$

In this equation, the ratio  $\frac{I_0}{I_Q}$  depicts the fluorescence intensity in absence of the quencher divided by the fluorescence intensity in presence of the quencher,  $K_{SV}$  is the Stern-Volmer constant for non-dynamic quenching (Lakowicz, 2006), and  $c_Q$  is the concentration of the quencher. Further information regarding LIF in multiphase systems, calibration methods and applications can be found in Rüttinger et al., 2018 (b).

## Data processing

Since it is the aim of this study to obtain information as close to the interface as possible, careful data processing is necessary. Close to the bubble surface, the tangential velocity  $v_\phi$  is of high interest. While at a fluidic interface (FI) the boundary condition for the radial velocity  $v_r$  is the same as at a solid interface (SI), the boundary condition for the tangential velocity  $v_\phi$  can be different from the solid interface.

This arises due to the mobile interface of the bubble (Clift et al., 2005). As a result of that, also the tangential velocities in proximity of a fluidic interface are different from those in proximity of a solid interface. To make statements about the convective motions close to the interface, the tangential velocity is calculated from the PIV data ( $v_x$  and  $v_y$ ) the following:

$$v_\phi = v_x \sin \phi - v_y \cos \phi$$

It is plotted for the interval

$$0 \leq \phi \leq 180^\circ$$

The nomenclature is illustrated in figure 3, where  $v_\infty$  depicts the mean velocity within the duct.

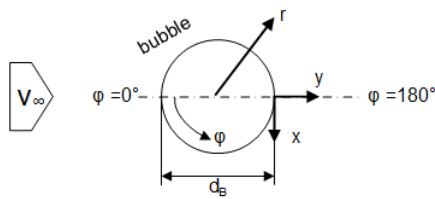


Fig. 3: Nomenclature of the single bubble (Rüttinger et al., 2018).

Mass transfer close to the interface is calculated by using the grey level gradients close to the interface recorded via Laser-induced Fluorescence. By means of the gradients, local Sherwood numbers can be determined which can be interpreted as dimensionless mass transfer coefficients. When the film theory is applied, the Sherwood number  $Sh$  can be calculated from the ratio of the characteristic length, which is the bubble diameter  $d_B$ , and the film thickness  $\delta$ , which is determined from the LIF images:

$$Sh = \frac{d_B}{\delta}$$

## Results and Discussion

In figures 4 and 5, the velocity profiles calculated from PIV data are presented. While in figure 4, the mean values are shown, in figure 5, the root mean square values (the standard deviation which depicts the velocity fluctuation and is known from turbulent flows) are plotted. Temporal averaging is carried out over 20 s, which is 10,000 images (see table 1). It is visible that in absence of a cylinder (empty items), a clear peak of the tangential velocity occurs at  $\varphi \approx 45^\circ$ . There, the fluid is accelerated due to the curved interface. At angles larger than  $\varphi \approx 110^\circ$ , the velocity is very low due to the bubble wake. The rms velocity profile does not have this steep gradients (figure 5).

In presence of a cylinder (grey filled items), the tangential velocity distribution does not have a sharp peak any more. It furthermore appears to be lower. This can be explained by the fact that behind the cylinder, the fluid is decelerated. Thus, the liquid from the cylinder wake approaching the bubble can have a lower mean velocity. But interestingly, while the mean velocity profile is lower, the rms velocity profile is significantly changed due to the vortex street. It is over all higher than in absence of the cylinder wake, and particularly higher for front part of the bubble  $\varphi \approx 0 \dots 90^\circ$ . This shows that the vortices generated by a flow around the cylinder approach the bubble and thus, change the flow structure in close proximity to it.

What is apparent for all the profiles visible in figure 4 and 5 is the fact that at the stagnation point ( $\varphi \approx 0^\circ$ ), the tangential velocity does not equal zero. This can be an indication that the liquid flow does not approach the bubble perpendicularly. This effect is enhanced by the cylinder whose center is not in one line with the bubble center so that the transient shear layer of the cylinder wake approaches the bubble.

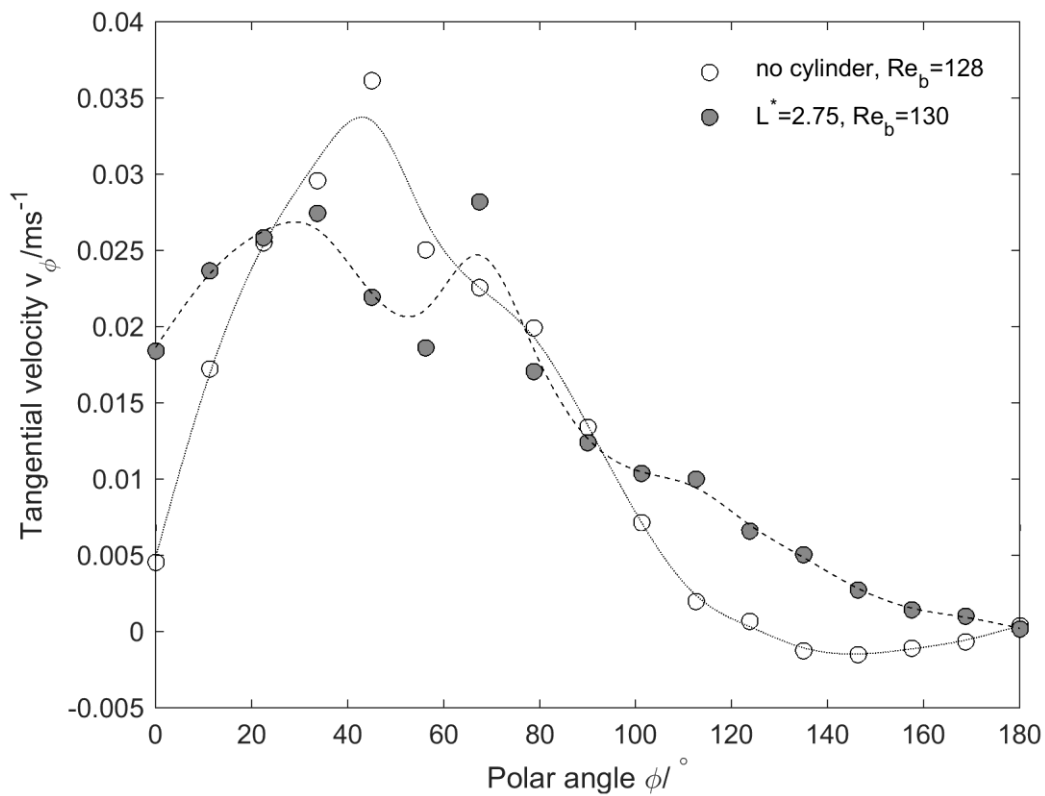


Fig. 4: Tangential mean velocity close to the fluidic interface of a CO<sub>2</sub> bubble in demineralized water (Sc=528).

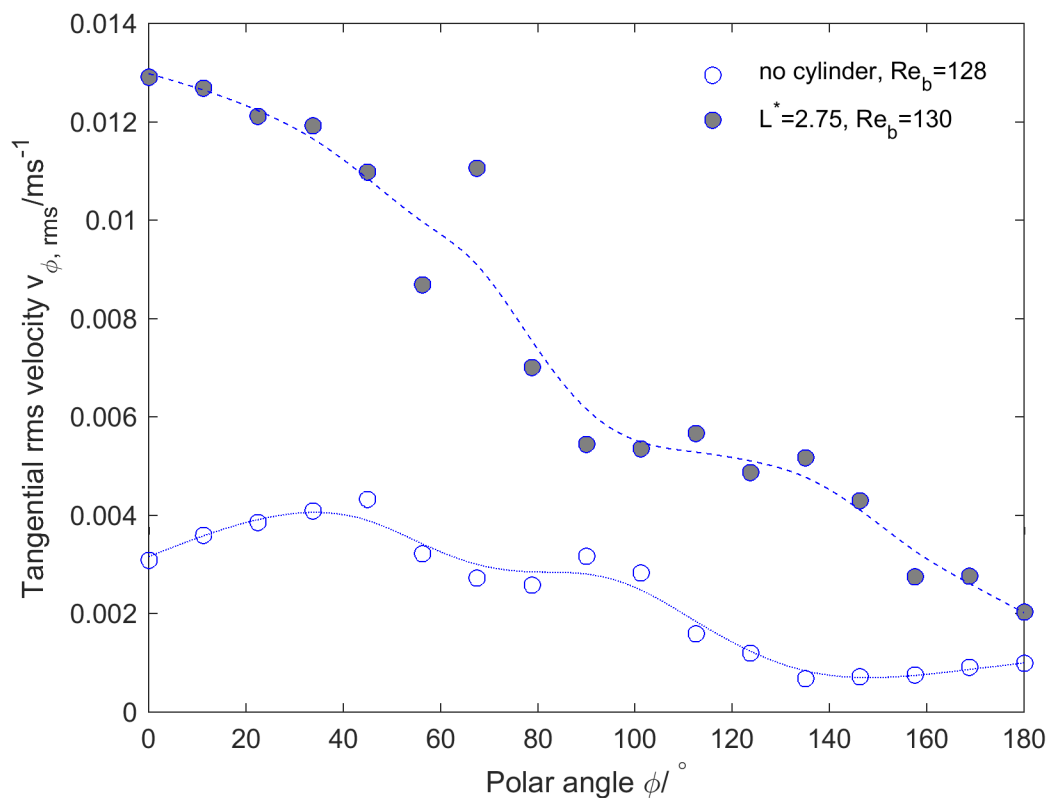


Fig. 5: Tangential root mean square velocity close to the fluidic interface of a CO<sub>2</sub> bubble in demineralized water (Sc=528).

The changed flow structure in proximity of the bubble raises the question whether the convective motions evoked by the vortices influence the mass transfer from the bubble into the bulk phase. To answer this question, local Sherwood numbers are calculated from the LIF images. The film thickness is estimated and, by means of the bubble diameter as a characteristic length, converted into the Sherwood number for nine different angles (see figure 3 for nomenclature).

In absence of a cylinder, the minimal Sherwood number is reached at an angle of  $\varphi \approx 110^\circ$  (empty items, figure 6). There, the film thickness reaches its maximum and the concentration boundary layer is detached from the bubble surface. A comparison with figure 4 shows that after accelerated fluid has passed the bubble, the concentration boundary layer is detached, and from this point, the tangential velocities are very close to zero or even negative (which indicates back flow at the rear part of the bubble). In presence of a cylinder, the local Sherwood numbers are lower which can be a result of the lower velocities close to the bubble. The minimum is now found at the very rear of the bubble, close to  $\varphi \approx 160^\circ$ . This implies that the concentration boundary layer is peeled off by the vortices and is detached further downstream.

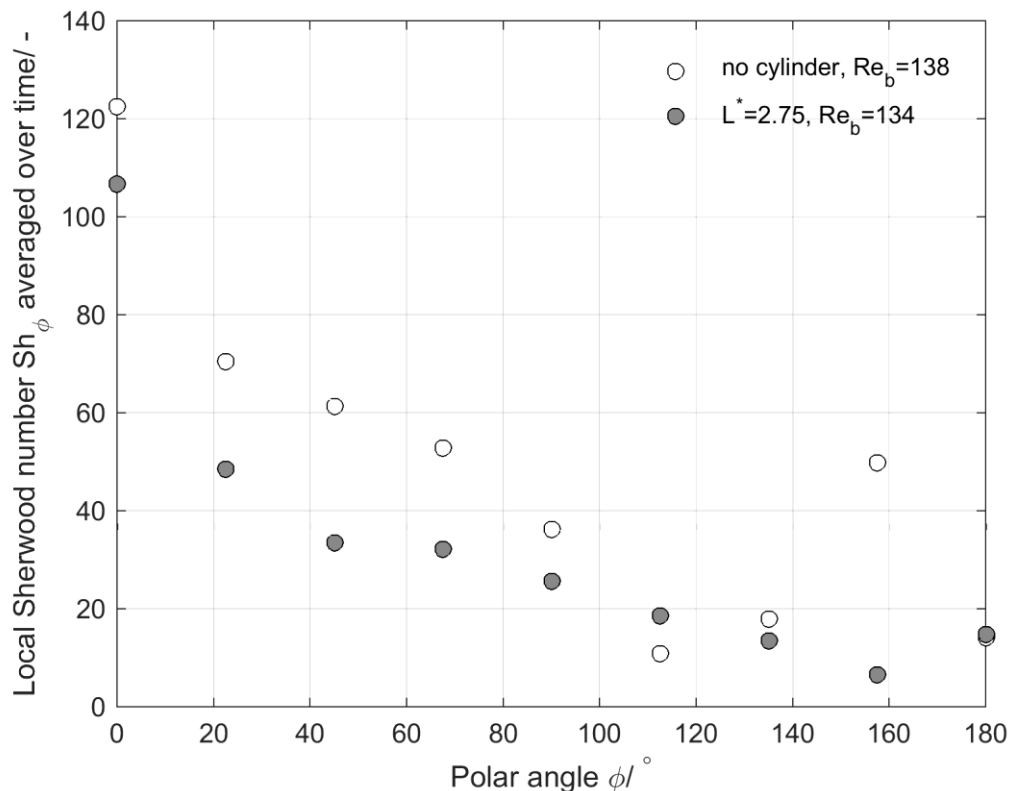


Fig. 6: Local Sherwood numbers of a  $\text{CO}_2$  bubble in demineralized water ( $Sc=528$ ).

Although there are locally different patterns observable depending on the presence of a cylinder, it is found that the global mass transfer which is calculated from the bubble shrinking rate (see Kastens et al., 2015), does not change. The global Sherwood number is for both cases (with and without cylinder) determined as  $Sh \approx 35$ . The explanation for this fact is that the vortices from the cylinder wake do not contain enough kinetic energy to influence the mass transfer significantly. Although they are able to peel off the concentration boundary layer which can be visualized by LIF measurements, this does not influence the limiting step in the mass transfer process, which is the diffusion. It is therefore concluded that the film

known from the film theory does not equal the concentration boundary layer from the LIF measurements. While the concentration boundary layer containing transferred species remaining close to the fluidic interface is comparably mobile and adapts to convective motions, the film itself is considered to be thinner and more stagnant, similar to the viscous sublayer in turbulent flows.

## Acknowledgements

The authors gratefully acknowledge the support which was given by the German Research Foundation (Deutsche Forschungsgemeinschaft: DFG) within the priority program SPP1740 under grant number SCHL 617/12-2.

## References

**Clift, R., Grace, J. R., Weber, M. E., 2005:** "Bubbles, drops, and particles". Dover Publications, Mineola, N. Y., republication from of the work first published by Academic Press, Inc., N. Y., in 1978.

**Kastens, S., Hosoda, S., Schlüter, M., Tomiyama, A., 2015:** "Mass transfer from Single Taylor Bubbles in Minichannels", *Chemical Engineering Technology*, Vol. 38(11): 1925-1931.

**Lakowicz, J. R., 2006:** *Principles of Fluorescence Spectroscopy*, 3rd ed., Springer US, Boston, MA.

**Lewis, W.K. and Whitman, W.G. 1924:** "Principles of Gas Absorption", *Industrial & Engineering Chemistry*, 16 (12):1215–1220.

**Rüttinger, S., Hoffmann, M., Schlüter, M., 2018:** "Experimental Analysis of a Bubble Wake Influenced by a Vortex Street". *Fluids*, 3, 8.

**Rüttinger, S., Spille, C., Hoffmann, M., Schlüter, M., 2018 (b):** "Laser-induced Fluorescence in Multiphase Systems", *ChemBioEng Reviews*, accepted for publication.

**Sumner, D., 2010:** "Two circular cylinders in cross-flow: A review". *Journal of Fluids and Structures*, 26(6):849–899.

**Zdravkovich, M.M., 1997:** "Flow around circular cylinders: Vol 1: Fundamentals". Oxford University Press, New York.